Oxidation of Germa- and Stanna-closo-dodecaborate

Journal:	*Dalton Transactions*
Manuscript ID:	DT-ART-01-2015-000099.R1
Article Type:	Paper
Date Submitted by the Author:	26-Jan-2015
Complete List of Authors:	Wesemann, Lars; University of Tuebingen, Institut fur Anorganische Chemie Gädt, Torben; University of Tübingen, Dimmer, Lörg-Alexander; University of Tübingen, Fleischhauer, Sebastian; University of Tübingen, Frank, Anita; University of Tübingen, Nickl, Claudia; University of Tübingen, Wütz, Tobias; University of Tübingen, Eichele, Klaus; University of Tübingen,

Oxidation of Germa- and Stanna-*closo*-dodecaborate

Torben Gädt,[a] Jörg-Alexander Dimmer,[a] Sebastian Fleischhauer,[a] Anita Frank,[a] Claudia Nickl,[a] Tobias Wütz,[a] Klaus Eichele,[a] and Lars Wesemann[a*]

Table of contents entry

Oxidation of group 14 heteroborates $[GeB_{11}H_{11}]^{2-}$ and $[SnB_{11}H_{11}]^{2-}$ yields a symmetrical dimer exhibiting a Ge–Ge bond or an unsymmetrical dimer bearing an Sn–B bond.

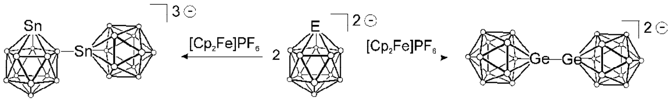

Journal Name RSCPublishing

ARTICLE

Oxidation of Germa- and Stanna-*closo*-dodecaborate

Cite this: DOI: 10.1039/x0xx00000x

Torben Gädt,[a] Jörg-Alexander Dimmer,[a] Sebastian Fleischhauer,[a] Anita Frank,[a] Claudia Nickl,[a] Tobias Wütz,[a], Klaus Eichele,[a] and Lars Wesemann[a]*

Received 00th January 2012,
Accepted 00th January 2012

DOI: 10.1039/x0xx00000x

www.rsc.org/

The oxidation of *closo*-heteroborates $[GeB_{11}H_{11}]^{2-}$ and $[SnB_{11}H_{11}]^{2-}$ is presented. Upon oxidation germa-*closo*-dodecaborate yields a symmetrical dimer exhibiting a Ge–Ge bond between two clusters. This dimer shows sulphur insertion into the Ge–Ge bond at room temperature. In contrast, oxidation of the homologous tin cluster results in an unsymmetrical dimer bearing an Sn–B bond between two clusters. The Sn–B dimer is also the product of the hydride abstraction reaction. In the presence of the donor ligand 2,2′-bipyridine, the oxidation of *closo*-cluster $[SnB_{11}H_{11}]^{2-}$ leads to the Sn(IV)-half sandwich coordination compound [bipy-$SnB_{11}H_{11}$] which dissolves in DMSO to give the Sn(IV)-adduct [bipy(DMSO)-$SnB_{11}H_{11}$].

Introduction

Heteroborane cluster chemistry is an active field of research and many interesting studies have been published in recent years.[1-10] In heteroborane clusters a BH vertex of a borane cluster skeleton is replaced by a main group element or a transition metal. Following the isolobal principle a BH unit can for example be substituted by a Ge atom or an anionic BH^- unit by an N atom respectively.[11-13] In these cases the resulting heteroboranes do not have a substituent but a lone pair at the vertex of the heteroelement and therefore can potentially act as a Lewis base. For more than ten years we have been interested in the chemistry of group 14 heteroborane clusters carrying an unsubstituted group 14 element like germanium or tin.[14] The monoheteroborane and diheteroborane clusters are the focus of our investigations with respect to synthesis, ligand properties in coordination chemistry and reactions with chalcogenes.[13-22] Besides their chemistry the NMR spectroscopical properties in solution and in the solid state were also explored. Furthermore the Mössbauer spectroscopy results of the tin clusters and their derivatives were published.[23] Due to the low oxidation state II of the group 14 elements in the clusters $[GeB_{11}H_{11}]^{2-}$ and $[SnB_{11}H_{11}]^{2-}$ we started to study oxidation reactions of these *closo*-heteroborates. The oxidation of the stanna-*closo*-dodecaborate $[SnB_{11}H_{11}]^{2-}$ with typical oxidation agents like hydrogen peroxide and iodine was investigated several years ago.[23, 24] The dianionic tin cluster $[SnB_{11}H_{11}]^{2-}$ reacts with hydrogen peroxide to give a tetrameric oxide $K_8[(OSnB_{11}H_{11})_4]$ (Chart 1).[23]

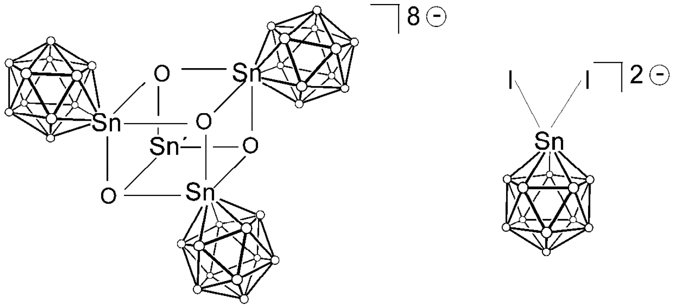

Chart 1 Two oxidation products of stanna-*closo*-dodecaborate (Sn′= [$SnB_{11}H_{11}$]).

In this heterocubane type structure three oxygen atoms coordinate at each tin vertex and the tin atom exhibits a very small isomeric ^{119}Sn Mössbauer shift indicating the oxidation state IV. In the case of the reaction of the cluster $[SnB_{11}H_{11}]^{2-}$ with iodine at –78°C we found oxidative addition of the halogen at the tin vertex of the cluster.[24] In this manuscript we present oxidation chemistry of germa- and stanna-*closo*-dodecaborate leading to unexpected Sn–B bond formation in the case of the tin cluster.

Results and discussion

In order to investigate the oxidation of germa-*closo*-dodecaborate $[GeB_{11}H_{11}]^{2-}$ we reacted a sample of the salt **1** with various oxidizing agents like hydrogen peroxide, iodine and ferrocenium hexafluorophosphate (Scheme 1).

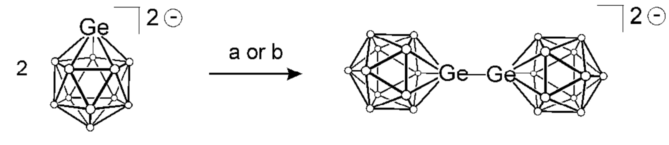

$[Bu_3MeN]_2[GeB_{11}H_{11}]$ (**1**) $[Bu_3MeN]_2[(GeB_{11}H_{11})_2]$ (**2**)

Scheme 1 Oxidation of germa-*closo*-dodecaborate, a: I_2, b: 2 $[Cp_2Fe][PF_6]$.

We were not able to characterize the product of the reaction of *closo*-cluster **1** with hydrogen peroxide. The ^{11}B NMR spectrum shows a new substance but due to the lack of crystalline material we cannot identify the composition of the product. However, in the case of the reaction with iodine or ferrocinium hexafluorophosphate the dimeric oxidation product **2** was formed quantitatively and isolated as colourless crystals (Scheme 1). The molecular structure together with selected interatomic distances is presented in Figure 1.[25] In the solid state structure of **2** we found two independent dimeric germaborate salts with one dianion lying on a centre of symmetry. Therefore we can discuss two independent Ge–Ge distances.

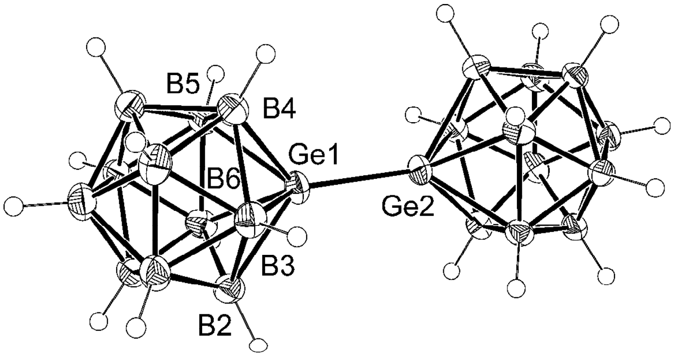

Fig. 1 Molecular structure of the oxidation product **2** in the solid state (ellipsoids set at 50% probability, distance in the second molecule in brackets). Tributylmethyl ammonium cations are omitted for the sake of clarity. Selected bond lengths [Å]: Ge1–B2 2.086(2), Ge1–B3 2.087(2), Ge1–B4 2.094(2), Ge1–B5 2.098(2), Ge1–B6 2.100(2), Ge1–Ge2 2.329(1) [2.340(1)].

To our surprise the observed Ge–Ge bond lengths of 2.329(1) [2.340(1)] Å are in the range of reported double bond values: 2.347(2) Å $[Ge_2R_4]$ [R = $CH(SiMe_3)_2$], 2.3026(3) Å $[Ar'HGe]_2$ [$Ar' = C_6H_3$-2,6(C_6H_3-2,6-$^iPr_2)_2$], 2.3173(3) Å [Ge(R)C_6H_3-2,6-$Trip_2]_2$ (R = Me, Et, Ph, Cl).[26-28] For the interpretation of the Ge–Ge bond length we use arguments of quantum chemical investigations which were published in the case of the chalcogen compounds of stanna- and germa-*closo*-dodecaborate.[23, 29] The Ge–Ge bonding interaction is mainly a single bond which might be enhanced as bonding and antibonding contributions of filled π and π* orbitals do not cancel exactly. As discussed in the chalcogen adducts, some of the π* orbitals might be slightly pushed away from the Ge atom in the direction of the cluster skeleton. In this fashion the radial antibonding character of these orbitals is weakened and the bond is strengthened.[23, 29] This type of delocalization of the antibonding orbitals on the borane cluster skeleton could be the reason for the short Ge–Ge bond although electrostatic repulsion between the two cluster units of the dianion should actually lengthen the said bond. Reduction of the dimer with NaH in thf leads to the starting material **1** in quantitative yield.

Dimer **2** still exhibits reactivity at the germanium atoms. At room temperature the cluster salt **2** was reacted with an excess of sulphur (Scheme 2) and after three days the sulphur insertion product **3** was isolated as colourless crystals. In Figure 2 the structure of the dianion in the solid state together with selected interatomic distances and angles is shown.

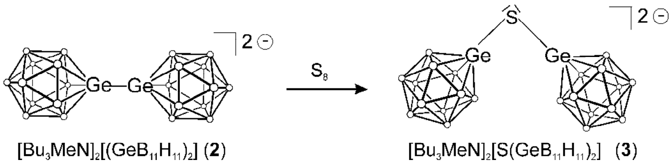

Scheme 2 Insertion of sulphur into the Ge–Ge bond of **2**.

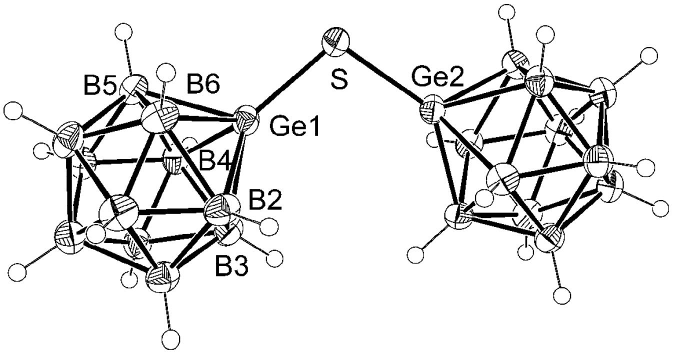

Fig. 2 Molecular structure of the sulphur insertion product **3** in the solid state (ellipsoids set at 50% probability). Tributylmethyl ammonium cations are omitted for the sake of clarity. Selected bond lengths [Å] and angles [°]: Ge1–B1 2.088(3), Ge1–B2 2.090(3), Ge1–B3 2.093(3), Ge1–B4 2.093(3), Ge1–B5 2.096(3), Ge1–S 2.178(1), Ge2–S 2.185(1), Ge1–S–Ge2 105.05(3).

The observed Ge–S separations of 2.178(1) and 2.185(1) Å are slightly longer than the Ge–S bond characterized in the sulphur adduct $[H_{11}B_{11}Ge\text{–}S]^{2-}$ of 2.102(1) Å. The found Ge–S–Ge structural motive is known in the literature from a variety of cyclic Ge-S structures but should only be compared with molecules showing a related sulphur bridge between two germanium moieties. These examples show longer Ge–S bond lengths and a comparable Ge–S–Ge angle: $[S(Ge\{CH_2Ph\}_3)_2]$ 2.235(21) Å, 111.0°; $[S\text{–}(GePh_3)_2]$ 2.212(1), 2.261(1), 2.227(2), 2.240(2) Å, 111.2(1), 110.7(1)°; $[\{Ge(S)[N(SiMe_3)C(Ph)C(SiMe_3)(C_5H_4N\text{-}_2)]\}_2S]$ 2.222(3), 2.226(3) Å, 101.4(1)°; $[S(Ge\{ButC(NAr)\}_2)_2]$, (Ar = 2,6-$iPr_2C_6H_3$) 2.2512(14), 2.2626(14) Å, 101.37(6)°; $[S\{Ge(NSiMe_3Ar)\}_2]$ (Ar = $C_6H_2(CHPh_2)_2Me$-2,6,4) 2.2854(8), 2.2869(8) Å, 98.21(3)°.[30-34]

In analogy to the oxidation of the germanium cluster **1** the reaction of the homologous tin cluster $[SnB_{11}H_{11}]^{2-}$ with the ferrocinium salt $[Cp_2Fe][PF_6]$ was also investigated. To our surprise we did not isolate a homologous dimer showing a Sn–Sn bond from this reaction. Instead a dimer exhibiting a Sn–B bond was formed (Scheme 3). Dimer **5** was characterized by elemental analysis, mass spectrometry and heteronuclear NMR spectroscopy. Although many different countercations were applied in the crystallization, crystals yielding suitable X-ray data for publication were not obtained. In the solution of the crystal structure determination a severe disorder of the trianion $[SnB_{11}H_{10}\text{-}(SnB_{11}H_{11})]^{3-}$ prevents a discussion of interatomic distances.

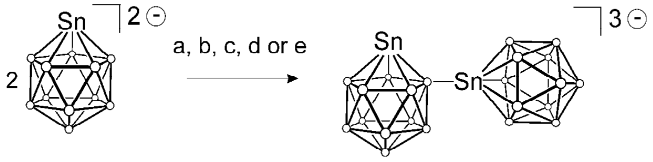

$[Et_3NH]_2[SnB_{11}H_{11}]$ (**4**) $[Et_3NH]_3[(SnB_{11}H_{10})(SnB_{11}H_{11})]$ (**5**)

Scheme 3 Oxidation of stanna-*closo*-dodecaborate to dimer **5**. The following reagents are possible: a, 2 $[Cp_2Fe][PF_6]$; b, 2 $PhI(OAc)_2$; c, Air; d, 1 $[CPh_3][BF_4]$ or e, 1 $[B(C_6F_5)_3]$.

The $^{119}Sn\{^1H\}$ NMR spectrum of **5** shows two characteristic signals at –267 [q] and –558 [s] ppm respectively. The non-binomial quartet at –267 ppm shows coupling to a ^{11}B atom with a $^1J(^{119}Sn\text{-}^{11}B)$ coupling constant of 850 Hz which is indicative of a direct Sn–B bond.[35] The singlet at –558 ppm is in a range comparable to the starting material **4** which shows a signal at –546 ppm.[15, 16, 36, 37] Due to the low symmetry of the trianion **5**, the $^{11}B\{^1H\}$ NMR spectrum exhibits eight signals with an intensity ratio of 1:1:1:2:2:2:2:11. Assignment of the signals was carried out on the basis of $^{11}B\{^1H\}$, ^{11}B NMR and $^{11}B\{^1H\}\text{-}^{11}B\{^1H\}$ COSY spectra. The oxidation product **5** was also formed in reaction with air or phenyl iodonium diacetate.

Since the formation of the trianion **5** can also be regarded as a hydride abstraction followed by nucleophilic attack of a $[SnB_{11}H_{11}]^{2-}$ cluster we studied the reaction of stanna-*closo*-dodecaborate with the Lewis acids $[B(C_6F_5)_3]$ and $[CPh_3][BF_4]$. Interestingly, with both reagents the Sn–B dimer **5** can be synthesized quantitatively.

In order to get further information about the oxidation pathways of the tin cluster the oxidation was also investigated in presence of donor ligands. In this reaction an acetonitrile solution of two equivalents of the oxidizing reagent were added to an acetonitrile solution of 2,2′-bipyridine and $[Bu_3MeN]_2[SnB_{11}H_{11}]$ (Scheme 4). Immediately a light brown precipitate was formed which was isolated by filtration. The solid is insoluble in common solvents except DMSO (vide infra). Elemental analysis confirms the formation of the bipy adduct **6** $[(bipy)SnB_{11}H_{11}]$. The ^{119}Sn MAS NMR spectrum which shows a resonance at –146 ppm (Figure 3) corroborates this finding since the comparable Sn(IV) cluster $[Me\text{–}SnB_{11}H_{11}]^-$ shows a resonance at –197 ppm whereas the chemical shift of $[SnB_{11}H_{11}]^{2-}$ is –546 ppm.[15, 16, 37]

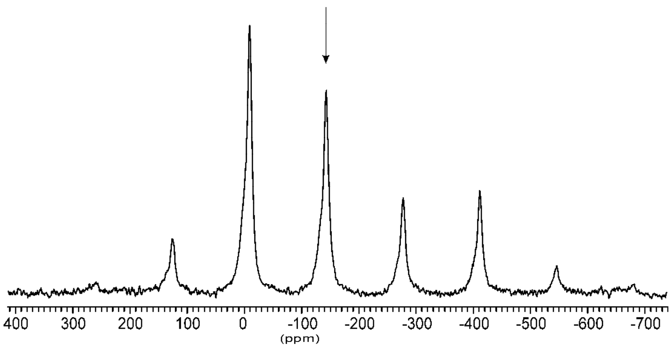

Fig. 3 Solid state ^{119}Sn VACP/MAS NMR spectrum of **6** obtained at 4.7 T and a spinning rate of 10 kHz, the isotropic peak is indicated by an arrow.

Upon dissolving the oxidation product **6** in DMSO at room temperature the solution turns red and the DMSO adduct **7** is formed (Scheme 5). After one day orange red crystals of **7** were isolated and characterized by single crystal diffraction, elemental analysis and NMR spectroscopy. The molecular structure of **7** is depicted in Figure 4 together with selected interatomic distances and angles. The tin vertex is centered above the pentagonal B5-face with Sn–B distances of 2.305(4) – 2.328(4) Å. These interatomic Sn–B distances are shorter than the distances found in $[(OSnB_{11}H_{11})_4]^{8-}$ [Sn–B range: 2.337(5) – 2.390(5)Å] and also shorter than the Sn–B values found in the starting material [2.381(4) – 2.389(3)Å].[23, 37] The tin vertex is coordinated with two exo-polyhedral ligands, viz. bipyridine and a DMSO molecule that is bonded to the tin vertex via its oxygen atom. The Sn–N separations are 2.241(3) and 2.233(3) Å respectively. Compared to the Sn(II)–N distances in 1-(2,2′-bipy)-2,3-Me_2-1-Sn-2,3-$C_2B_9H_9$ [2.412(14), 2.374(15) Å] and 1-Sn(bipy)-2,3-$(SiMe_3)_2$-2,3-$C_2B_4H_4$ [2.49(1), 2.54(1)] the Sn–N distances of **7** are remarkably short.[38, 39] Further references from known bipyridine adducts of Sn(IV) species like $[Me(Ph)SnCl_2(bipy)]$ [Sn–N 2.389, 2.401 Å] and $[MeCl_2(bipy)Sn(CH_2)SnCl_2Me]$ [Sn–N 2.270, 2.372 Å] corroborate the finding that adduct **7** exhibits rather short Sn–N distances.[40, 41] The tin oxygen separation amounts to 2.266(2) Å which is a reasonable value compared to literature known distances between an Sn(IV) center and a DMSO ligand.[42-44]

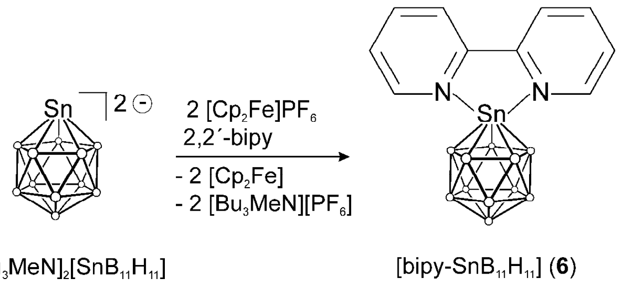

$[Bu_3MeN]_2[SnB_{11}H_{11}]$ $[bipy\text{-}SnB_{11}H_{11}]$ (**6**)

Scheme 4 Oxidation of $[SnB_{11}H_{11}]^{2-}$ and reaction with 2,2′-bipy.

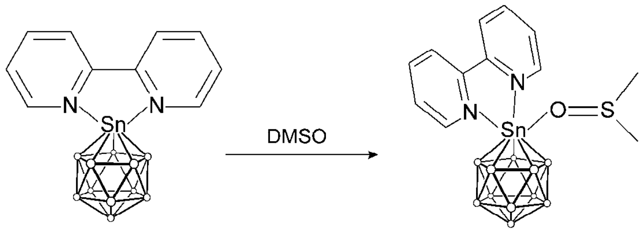

$[bipy\text{-}SnB_{11}H_{11}]$ (**6**) $[bipy(DMSO)\text{-}SnB_{11}H_{11}]$ (**7**)

Scheme 5 Reaction of the bipy adduct **6** with DMSO.

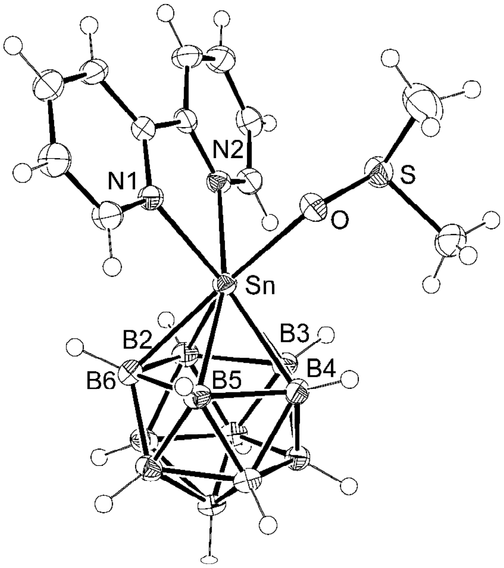

Fig. 4 Molecular structure of the DMSO adduct **7** (ellipsoids set at 50% probability) in the solid state. Selected bond lengths [Å] and angles [°]: B2–Sn 2.305(4), B3–Sn 2.328(4), B4–Sn 2.319(4), B5–Sn 2.314(4), B6–Sn 2.317(4), N1–Sn 2.241(3), N2–Sn 2.233(3), O–Sn 2.266(2), O–S 1.562(3), N1–Sn–N2 72.6(1), N2–Sn–O 78.8(1), N1–Sn–O 78.2(1).

Compound **7** can also be viewed as a rare example of an η^5-coordinated Sn(IV) atom which has not been documented for many ligands. Hosmane presented a rare example for a bent-sandwich complex of Sn(IV) with a carborane ligand.[45, 46] With the DMSO adduct **7** we have isolated the second example for a half sandwich complex of type $[L_3Sn(B_{11}H_{11})]$. The tetrameric oxide $[(OSnB_{11}H_{11})_4]^{8-}$ (Chart 1) is another example for this type of coordination. Formally these molecules can be separated into a $L_3Sn(IV)$ fragment coordinated at a $[B_{11}H_{11}]^{4-}$ ligand which is isolobal with the carbollide $[C_2B_9H_{11}]^{2-}$ and cyclopentadienide $[Cp]^-$ ligand.[47] We would also like to discuss the presented heteroborates **6** and **7** with respect to Wade´s cluster rules.[48] According to these rules the donor ligands contribute two electrons each to the electron count of the tin vertex and thus the tin vertex contributes in the case of **6** six and in the case of **7** eight electrons to the cluster count. In addition to the eleven BH-fragments which contribute 22 electrons both clusters exhibit an electron count higher than the 26 electrons necessary for a twelve vertex *closo* cluster. However both molecules **6** and **7** show an icosahedral twelve vertex *closo* geometry.[49] Obviously, the canonical Wade counting scheme fails to predict the correct cluster structures in the case of oxidized stanna-*closo*-dodecaborate species with main group element ligands.

Experimental

General: All manipulations were carried out under argon in Schlenk glassware. Solvents were dried and purified by standard methods and stored under Argon. NMR spectra were recorded with a Bruker DRX-250 operating at 250.13 (^{1}H), 80.25 (^{11}B), 62.9 (^{13}C), 101.25 (^{31}P) and 93.25 MHz (^{119}Sn) and a Bruker AvanceII+500 NMR-spectrometer (^{1}H, 500.13 MHz; ^{13}C, 125.76 MHz; ^{119}Sn, 186.50 MHz). Chemical shifts are reported in δ values in ppm relative to external TMS (^{1}H, ^{13}C) $BF_3{*}Et_2O$ (^{11}B) or $SnMe_4$ (^{119}Sn) using the chemical shift of the solvent ^{2}H resonance frequency. The solid-state ^{119}Sn CP/MAS spectra were obtained at 74.63 MHz using a Bruker DSX-200 spectrometer (B_0 = 4.7 T). Powdered samples of **6** were packed into 4 mm zirconia rotors. After cross-polarization (CP) the spectra were acquired under high-power proton decoupling and were referenced with respect to external $SnMe_4$ *via* external $SnCy_4$ at –97.4 ppm. Elemental analyses were performed at the Institut für Anorganische Chemie, University of Tübingen using a Vario EL analyzer.

Crystallography: X-Ray data for compounds **3** and **7** were collected on a Stoe IPDS 2T diffractometer and were corrected for Lorentz and polarization effects and absorption by air. The programs used for **3** and **7** are Stoe's X-Area and the WinGX suite of programs including SHELXS and SHELXL for structure solution and refinement.[50, 51-53] Numerical absorption correction based on crystal shape optimization was applied for all compound with Stoe's X-Red and X-Shape.[54, 55] X-Ray data for **2** were collected with a Bruker APEX-II CCD diffractometer equipped with a sealed tube source with molybdenum anode and graphite monochromator. For data reduction and absorption correction Bruker´s APEX2[56] including the programs SAINT, [57] SADABS[58] and XPREP was used.[59]

Synthesis of $[Bu_3MeN]_2[(GeB_{11}H_{11})_2]$ (2): To a solution of $[Bu_3MeN]_2[GeB_{11}H_{11}]$ (100 mg, 0.160 mmol) in acetonitrile (10 mL), I_2 (21 mg, 0.08 mmol) was added as a solid. The colour of the reaction mixture vanished rapidly. After stirring for one hour, all volatile components were removed under reduced pressure. The residue was washed with water to remove $[Bu_3MeN]I$ and the solid was dried overnight. Colourless crystals of **2** (39 mg, 60 % yield) were obtained by layering a filtered solution of the residue in dichloromethane with *n*-hexane. ^{1}H NMR (250.13 MHz, CD_2Cl_2) *δ*: 0.94 [t, $^3J(^1H\text{-}^1H)$ = 7.3 Hz, 18H, CH_2CH_3], 1.36 (m, 12H, CH_2CH_3), 1.59 (m, 12H, $CH_2CH_2CH_2$), 2.92 (s, 6H, NCH_3), 3.08 ppm (m, 12H, NCH_2CH_2). ^{11}B{^{1}H} NMR (80.25 MHz, CD_2Cl_2) *δ*: –7.0 (s, 2B; B12), –14.5 ppm (s, 20B, B2-B11). Elemental analysis (%) calcd for $C_{26}H_{82}B_{22}Ge_2N_2$ (806.01 g/mol): C, 38.74; H, 10.25: N, 3.48. found: C, 38.85; H, 10.07; N, 3.49.

Synthesis of $[Bu_3MeN]_2[S(GeB_{11}H_{11})_2]$ (3): $[Bu_3MeN]_2[(GeB_{11}H_{11})_2]$ (**2**) (67 mg, 0.08 mmol) was dissolved in dichloromethane (12 mL). Excess sulphur was added as a solid and the reaction mixture was stirred for three days. The mixture was filtered and carefully layered with *n*-hexane. After several days, colourless crystals of **3** (35 mg, 50 % yield) were obtained. ^{11}B{^{1}H} NMR (80.25 MHz, CD_2Cl_2) *δ*: –13.7 (s, 2B, B12), –16.3 ppm (s, 20B, B2-B11). Elemental analysis (%) calcd for $C_{26}H_{82}B_{22}Ge_2N_2S$ (838.08 g/mol): C, 37.26; H, 9.86; N, 3.34; S, 3.83. found: C, 37.25; H, 9.17; N, 3.39; S, 3.74.

Synthesis of $[Et_3HN]_3[SnB_{11}H_{10}\text{-}SnB_{11}H_{11}]$ (5): 64.4 mg (0.200 mmol) $PhI(OAc)_2$ were dissolved in 10 mL acetonitrile and 1 mL H_2O was added. The solution was stirred for 30 minutes. 45.3 mg (0.100 mmol) $[Et_3HN]_2[SnB_{11}H_{11}]$ were added and the colour of the solution turns to bright yellow immediately. After stirring for two hours the colour had disappeared and all volatiles were removed in vacuum. The remaining residue was washed three times each with water and diethyl ether. The resulting colourless solid was dried in vacuum. Crystals were obtained by slow diffusion of diethyl ether into an acetonitrile solution of **5**. (31.7 mg, 79% yield)
Alternatively 45.3 mg (0.100 mmol) $[Et_3HN]_2[SnB_{11}H_{11}]$ were dissolved in 20 mL acetonitrile, two equivalents of

$[\mathrm{Cp_2Fe}][\mathrm{PF_6}]$ dissolved in 10 mL acetonitrile were added and the colour of the solution instantly turns to bright yellow. Volatiles were removed in vacuum and the remaining residue was washed with water and diethyl ether. The resulting colourless solid was dried in vacuum and recrystallized form acetonitrile by slow diffusion of diethyl ether. (25.0 mg, 62% yield). $^{1}\mathrm{H}\{^{11}\mathrm{B}\}$ NMR (250.13 MHz, $\mathrm{CH_3CN}$) δ: 1.27 [t, $^{3}J(^{1}\mathrm{H}\text{-}^{1}\mathrm{H}) = 7.3$ Hz 27H, $\mathrm{CH_3}$], 3.13 [q, $^{3}J(^{1}\mathrm{H}\text{-}^{1}\mathrm{H}) = 7.3$ Hz, 18H, N-$\mathrm{CH_2}$-], $^{11}\mathrm{B}\{^{1}\mathrm{H}\}$ NMR (160.46 MHz, $\mathrm{CH_3CN}$) δ: –3.6 (B12), –8.0 (B9), –8.6 (B4/5), –10.0 (B3/6), –11.4 (B7/11, 8/10), –13.6 (B2), –15.8 ($\mathrm{SnB_{11}}$). $^{119}\mathrm{Sn}\{^{1}\mathrm{H}\}$ NMR (186.43 MHz, $\mathrm{CH_3CN}$) δ: –267 [q, $^{1}J(^{119}\mathrm{Sn}\text{-}^{11}\mathrm{B}) = 850$ Hz], –558 (s, br). Elemental analysis calcd (%) calcd for ($[\mathrm{Et_4N}]_3[\mathrm{SnB_{11}H_{10}}\text{-}\mathrm{SnB_{11}H_{11}}]$) $\mathrm{C_{24}H_{81}B_{22}N_3Sn_2}$ (803.03 g/mol): C, 32.49; H, 9.20; N, 4.74. found C, 32.14 H, 8.9, N, 4.71. ESI-MS (neg. mode): $\{[\mathrm{Et_4N}]_2[\mathrm{Sn_2B_{22}H_{21}}]\}^{-}$ calcd 756.5, found 756.5.

Synthesis of $[(\text{bipy})\text{-}\mathrm{SnB_{11}H_{11}}]$ (6): 260 mg (0.400 mmol) $[\mathrm{Bu_3MeN}]_2[\mathrm{SnB_{11}H_{11}}]$ and 62.5 mg (0.400 mmol) 2,2' bipyridine were dissolved in 10 mL acetonitrile. To the stirred solution was added dropwise a solution of 265 mg (0.800 mmol) $[\mathrm{FeCp_2}][\mathrm{PF_6}]$. The colour of the reaction mixture changed to orange-brown and a light brown precipitate was formed. The solid was filtered off, washed three times with 10 mL $\mathrm{CH_2Cl_2}$ and dried overnight. (85.8 mg, 53.0 % yield). IR (ATR): 2496 (s, ν(B-H)), 1013 (m, δ(B-H)), 767 (m, δ(C-H)), 720 (m, cage breathing), 288 (w, $\nu(\mathrm{H_{11}B_{11}Sn\text{-}N})$. Elemental analysis (%) calcd for $\mathrm{C_{10}H_{19}B_{11}N_2Sn}$ (404.91 g/mol): C, 29.32; H, 4.73; N, 6.92. found: C, 30.03; H, 4.61; N, 6.28.

Synthesis of $[(\text{bipy})\text{-}(\text{DMSO})\text{-}\mathrm{SnB_{11}H_{11}}]$ (7): 81 mg (0.20 mmol) $[(\text{bipy})\text{-}\mathrm{SnB_{11}H_{11}}]$ (**6**) were dissolved in a minimum amount of DMSO. Crystalline material formed within 24 hours and was collected via filtration. The solid was washed several times with $\mathrm{CH_2Cl_2}$ and MeOH and dried overnight under reduced pressure. (20.3 mg, 21.0% yield) $^{1}\mathrm{H}\{^{11}\mathrm{B}\}$ NMR (250.13 MHz, DMSO) δ: 9.2 (br, 2H, bipy), 9.00 (br, 2H, bipy), 8.63 (br, 2H, bipy), 8.18 (br, 2H, bipy), 1.50-0.70 (br, 11H, B-H). $^{11}\mathrm{B}\{^{1}\mathrm{H}\}$ NMR (80.25 MHz, DMSO) δ: –20.9 (br). $^{13}\mathrm{C}\{^{1}\mathrm{H}\}$ NMR (62.90 MHz, DMSO, δ): 159.0 (bipy), 139.2 (bipy), 128.1 (bipy), 124.5 (bipy). $^{119}\mathrm{Sn}\{^{1}\mathrm{H}\}$ NMR (93.25 MHz, DMSO) δ: –208 (br). Elemental analysis (%) calcd for $\mathrm{C_{12}H_{25}B_{11}N_2OSSn}$ (483.04 g/mol): C, 29.84; H, 5.22; N, 5.80; S, 6.64. found: C, 29.39; H, 5.33; N, 5.34; S, 6.11.

Conclusions

The homologous *closo*-clusters germa-*closo*-dodecaborate and stanna-*closo*-dodecaborate show different reaction products upon oxidation. Whereas germa-*closo*-dodecaborate forms a symmetrical dimer exhibiting a Ge–Ge bond as the product of oxidation the tin cluster reacts to an unsymmetrical dimer bearing an Sn–B bond. The Sn–B dimer is also the product of the hydride abstraction reaction of $[\mathrm{SnB_{11}H_{11}}]^{2-}$. Furthermore in the presence of donor ligands the oxidation of the *closo*-cluster $[\mathrm{SnB_{11}H_{11}}]^{2-}$ leads to Sn(IV) half sandwich coordination compounds of the type $[\mathrm{L_xSn(B_{11}H_{11})}]$ (x = 2-3).

Acknowledgements

Financial support of the Deutsche Forschungsgemeinschaft is gratefully acknowledged.

Notes and references

[a] Institut für Anorganische Chemie, Universität Tübingen, Auf der Morgenstelle 18, 72076 Tübingen, Germany.

1. D. Olid, R. Nunez, C. Vinas and F. Teixidor, *Chem. Soc. Rev.*, 2013, 42, 3318-3336.
2. R. S. Anju, K. Saha, B. Mondal, V. Dorcet, T. Roisnel, J.-F. Halet and S. Ghosh, *Inorg. Chem.*, 2014, 53, 10527-10535.
3. Y. Quan and Z. Xie, *J. Am. Chem. Soc.*, 2014, 136, 15513-15516.
4. B. Calvo, B. Roy, R. Macías, M. J. Artigas, F. J. Lahoz and L. A. Oro, *Inorg. Chem.*, 2014, DOI: 10.1021/ic501779n.
5. D. A. Wann, P. D. Lane, H. E. Robertson, J. Holub and D. Hnyk, *Inorg. Chem.*, 2013, 52, 4502-4508.
6. W. Y. Man, S. Zlatogorsky, H. Tricas, D. Ellis, G. M. Rosair and A. J. Welch, *Angew. Chem.*, 2014, 126, 12418-12421.
7. D. Ellis, G. M. Rosair and A. J. Welch, *Chem. Commun.*, 2010, 46, 7394-7396.
8. Y. Quan, Z. Qiu and Z. Xie, *J. Am. Chem. Soc.*, 2014, 136, 7599-7602.
9. J. Zhang and Z. Xie, *Acc. Chem. Res.*, 2014, 47, 1623-1633.
10. H. Scheel, J. Wiederkehr, K. Eichele, H. A. Mayer, F. Winter, R. Pottgen and L. Wesemann, *Dalton Trans.*, 2014, 43, 11867-11876.
11. D. Hnyk, M. Buehl, P. v. R. Schleyer, H. V. Volden, S. Gundersen, J. Mueller and P. Paetzold, *Inorg. Chem.*, 1993, 32, 2442-2445.
12. F. Meyer, J. Müller, P. Paetzold and R. Boese, *Angew. Chem.*, 1992, 104, 1221-1222.
13. C. Nickl, D. Joosten, K. Eichele, C. Maichle-Mössmer, K. W. Tornroos and L. Wesemann, *Angew. Chem., Int. Ed.*, 2009, 48, 7920–7923.
14. L. Wesemann, T. Marx, U. Englert and M. Ruck, *Eur. J. Inorg. Chem.*, 1999, 1563–1566.
15. T. Gädt and L. Wesemann, *Organometallics*, 2007, 26, 2474–2481.
16. T. Marx, B. Mosel, I. Pantenburg, S. Hagen, H. Schulze and L. Wesemann, *Chem.–Eur. J.*, 2003, 9, 4472–4478.
17. J.-A. Dimmer, M. Hornung, T. Wütz and L. Wesemann, *Organometallics*, 2012, 31, 7044-7051.
18. M. Kirchmann, K. Eichele, F. M. Schappacher, R. Pöttgen and L. Wesemann, *Angew. Chem., Int. Ed.*, 2008, 47, 963–966.
19. H. Schubert, J.-A. Dimmer, F. R. Küchle, K. Eichele and L. Wesemann, *Inorg. Chem.*, 2011, 50, 664–670.
20. J.-A. Dimmer, H. Schubert and L. Wesemann, *Chem.–Eur. J.*, 2009, 15, 10613–10619.
21. C. Nickl, K. Eichele, D. Joosten, T. Langer, F. M. Schappacher, R. Pöttgen, U. Englert and L. Wesemann, *Angew. Chem., Int. Ed.*, 2011, 50, 5766-5769.
22. D. Joosten, I. Pantenburg and L. Wesemann, *Angew. Chem., Int. Ed.*, 2006, 45, 1085–1087.
23. M. Kirchmann, T. Gädt, F. M. Schappacher, R. Pöttgen, F. Weigend and L. Wesemann, *Dalton Trans.*, 2009, DOI: Doi 10.1039/B814936d, 1055–1062.
24. T. Gädt, F. M. Schappacher, R. Pöttgen and L. Wesemann, *Inorg. Chem.*, 2007, 46, 2864–2869.
25. Details about the crystal structure solution are given in the Supporting Information.
26. G. H. Spikes, J. C. Fettinger and P. P. Power, *J. Am. Chem. Soc.*, 2005, 127, 12232-12233.
27. P. B. Hitchcock, M. F. Lappert, S. J. Miles and A. J. Thorne, *Chem. Commun.*, 1984, DOI: 10.1039/C39840000480, 480-482.
28. M. Stender, L. Pu and P. P. Power, *Organometallics*, 2001, 20, 1820-1824.
29. J.-A. Dimmer, M. Hornung, F. Weigend and L. Wesemann, *Dalton Trans.*, 2010, 39, 7504–7512.
30. C. Glidewell and D. C. Liles, *Acta Crystallogr., Sect. B: Struct. Sci.*, 1982, 38, 1320-1323.
31. B. Krebs and H.-J. Korte, *J. Organomet. Chem.*, 1979, 179, 13-23.
32. W.-P. Leung, W.-K. Chiu, K.-H. Chong and T. C. W. Mak, *Chem. Commun.*, 2009, DOI: 10.1039/B916326C, 6822-6824.
33. S.-H. Zhang and C.-W. So, *Organometallics*, 2011, 30, 2059-2062.

34. J. Li, M. Hermann, G. Frenking and C. Jones, *Angew. Chem., Int. Ed.*, 2012, 51, 8611-8614.
35. L. Barton and D. K. Srivastava, *Dalton Trans.*, 1992, DOI: 10.1039/DT9920001327, 1327-1328.
36. R. W. Chapman, J. G. Kester, K. Folting, W. E. Streib and L. J. Todd, *Inorg. Chem.*, 1992, 31, 979–983.
37. T. Gädt and L. Wesemann, *Z. Anorg. Allg. Chem.*, 2007, 633, 693–699.
38. P. Jutzi, P. Galow, S. Abu-Orabi, A. M. Arif, A. H. Cowley and N. C. Norman, *Organometallics*, 1987, 6, 1024-1031.
39. N. S. Hosmane, P. De Meester, N. Maldar, S. B. Potts, S. S. C. Chu and R. H. Herber, *Organometallics*, 1986, 5, 772-778.
40. M. A. Buntine, V. J. Hall, F. J. Kosovel and E. R. T. Tiekink, *J. Phys. Chem. A*, 1998, 102, 2472-2482.
41. M. Austin, K. Gebreyes, H. G. Kuivila, K. Swami and J. A. Zubieta, *Organometallics*, 1987, 6, 834-842.
42. R. García-Zarracino and H. Höpfl, *J. Am. Chem. Soc.*, 2005, 127, 3120-3130.
43. P. Álvarez-Boo, J. S. Casas, M. D. Couce, R. Farto, V. Fernández-Moreira, E. Freijanes, J. Sordo and E. Vázquez-López, *J. Organomet. Chem.*, 2006, 691, 45-52.
44. R. Krishnamurti, H. G. Kuivila, N. S. Shaik and J. Zubieta, *Organometallics*, 1991, 10, 423-431.
45. L. Jia, H. Zhang and N. S. Hosmane, *Organometallics*, 1992, 11, 2957-2959.
46. P. H. M. Budzelaar, J. J. Engelberts and J. H. van Lenthe, *Organometallics*, 2003, 22, 1562-1576.
47. U. Schneider and R. Ahlrichs, *Chem. Phys. Lett.*, 1994, 226, 491-494.
48. K. Wade, in *Advances in Inorganic Chemistry*, eds. H. J. Emeléus and A. G. Sharpe, Academic Press, 1976, vol. Volume 18, pp. 1–66.
49. L. Wesemann, Y. Ramjoie, M. Trinkaus, B. Ganter and J. Muller, *Angew. Chem., Int. Ed.*, 1998, 37, 1412–1415.
50. X-AREA 1.26, Stoe & Cie, Darmstadt, Germany, 2004.
51. L. J. Farrugia, *J. Appl. Crystallogr.*, 1999, 32, 837–838.
52. G. M. Sheldrick, Göttingen, Germany, 1997, p. Program for the Solution of Crystal Structures.
53. G. M. Sheldrick, Göttingen, Germany, 1997, p. Program of the Crystal Structure Refinement.
54. X-RED 1.26, Stoe & Cie, Darmstadt, Germany, 2004.
55. X-SHAPE 2.05, Stor & Cie, Darmstadt, Germany, 2004.
56. APEX2 v2011.8-0, Bruker AXS, Madison, WI, 2011.
57. SAINT V7.68A, Bruker AXS, Madison, WI, 2011.
58. SADABS V2008/1, BrukerAXS, Madison, WI, 2008.
59. Details about the crystal structure solution are given in the Supporting Information.

Oxidation of Germa- and Stanna-*closo*-dodecaborate

Torben Gädt,[a] Jörg-Alexander Dimmer,[a] Sebastian Fleischhauer,[a] Anita Frank,[a] Claudia Nickl,[a] Tobias Wütz,[a] Klaus Eichele,[a] and Lars Wesemann[a*]

Table of contents entry

Oxidation of group 14 heteroborates $[GeB_{11}H_{11}]^{2-}$ and $[SnB_{11}H_{11}]^{2-}$ yields a symmetrical dimer exhibiting a Ge–Ge bond or an unsymmetrical dimer bearing an Sn–B bond.